

CHROM. 20 581

## POST-CAPILLARY FLUORESCENCE DETECTION IN CAPILLARY ZONE ELECTROPHORESIS USING *o*-PHTHALDIALDEHYDE

DONALD J. ROSE, Jr. and JAMES W. JORGENSEN\*

*Department of Chemistry, University of North Carolina, Chapel Hill, NC 27599-3290 (U.S.A.)*

(Received March 16th, 1988)

---

### SUMMARY

A post-capillary fluorescence detection scheme for capillary zone electrophoresis is described using *o*-phthaldialdehyde (OPA) as the tagging reagent. Use of a coaxial capillary reactor affords mixing of the OPA reagent with migrating zones without excessive zone broadening. The detector is linear over three orders of magnitude and shows detection limits for amino acids and proteins in the femtomol (attomol) range.

---

### INTRODUCTION

Capillary zone electrophoresis (CZE) is a separation technique which resolves species according to their differential rate of migration through solution in the presence of an electric field. Use of a capillary provides efficient dissipation of heat which reduces the zone-broadening effects of convection. Use of a capillary, however, requires small sample sizes and thus the need for sensitive methods of detection.

Detection of zones in CZE can be done by monitoring zones either migrating within the capillary or emerging from the end of the capillary. Zone detection within the capillary has been accomplished by measuring changes in UV absorption<sup>1</sup>, fluorescence<sup>2,3</sup>, refractive index<sup>4</sup>, or conductivity<sup>5–7</sup> as the zone migrates past the point of detection. Because the detection “cell” is a portion of the electrophoresis capillary, these techniques are relatively simple to employ and result in minimal additional broadening of the measured zones. Detection of zones after they migrate from the end of the capillary is more difficult to employ. A connection must be made with the end of the capillary permitting current to flow during electrophoresis while not significantly perturbing and broadening the zone. Examples of this type of “post-capillary” detection include interfacing to a mass spectrometer<sup>8</sup> and an electrochemical (amperometric) detector<sup>9</sup>.

One area of application for CZE is the separation and characterization of amino acids, peptides and proteins. Of the detection methods previously mentioned, fluorescence detection offers the most sensitivity for this group of biological compounds and is usually accomplished by labelling the compound with a fluorescent “tag”. In liquid chromatography (LC), reagents such as fluorescein isothiocyanate

(FITC)<sup>10,11</sup>, fluorescamine<sup>12,13</sup>, dansyl chloride<sup>14,15</sup>, and *o*-phthaldialdehyde (OPA)<sup>16–18</sup>, have been used to label amine functional groups on biological compounds before the chromatographic separation. Alternatively, fluorescamine<sup>19,20</sup> and OPA<sup>21,22</sup> have been mixed with the chromatographic effluent stream to detect sample components following the chromatographic separation.

Use of the pre-separation labelling scheme for CZE has limitations. For example, OPA-labelled amino acids decompose over time with the rate of decomposition being amino acid-dependent<sup>23</sup>. Another limitation arises from the fluorescent tags changing the net charge on sample molecules and thus changing the mobility of the ion during the separation. For example, each FITC molecule replaces the positive charge of the amine on the tagged molecule with a negative charge due to the carboxylate on the fluorescein. This is not critical for compounds such as amino acids with one or two reactive amine groups, but for proteins, which have many amine groups (*e.g.* a terminal amine plus numerous lysine epsilon amines along the peptide chain), different protein molecules can possess a different number of tags. Unless all protein molecules are tagged to the same extent (*i.e.* they all have the same number of tags), each compound with a different number and/or arrangement of tags will have a different electrophoretic mobility and fluorescence intensity. In this way, a single protein can yield multiple peaks.

This article reports on the successful implementation of post-capillary detection in CZE with OPA as the labelling reagent. The introduction of reagent is accomplished using a coaxial capillary reactor consisting of two concentric fused-silica capillaries. The reactor dimensions are optimized for maximum signal with minimal zone broadening. In addition, the reactor is characterized in terms of linearity and detection limits and is compared to conventional UV absorption detection. Various applications will be shown for samples of biological significance.

## EXPERIMENTAL

### *Post-capillary reactor*

Fig. 1 shows a schematic cross-section of the post-capillary reactor. The reaction capillary, held in the stainless-steel tee (Swagelok, Crawford Fitting; Ontario, Canada) by Vespel ferrules, has a 1–2 cm wide window formed by burning off the polyimide coating. The electrophoretic capillary, with an outer diameter smaller than the inner diameter of the reaction capillary, passes through the tee and inserts into the reaction capillary such that the two capillaries are concentric and form the coaxial reactor. The reagent capillary enters the short arm of the tee and is secured by a ferrule. Fused-silica capillaries (Polymicro Technologies; Phoenix, AZ, U.S.A.), were used throughout the reactor. The inner and outer diameters of electrophoretic and reaction capillaries varied according to experimental design. The reagent capillary dimensions were constant throughout the study with an inner diameter of 200  $\mu\text{m}$ , an outer diameter of 325  $\mu\text{m}$ , and a length of approximately 70 cm.

Fig. 2 shows the post-capillary reactor as a part of the overall CZE experimental set-up. The electrophoretic and reaction capillaries each dip into leveled buffer reservoirs, containing the operating buffer, which are connected to the high voltage power supply by platinum electrodes. The tee is not connected to ground but is left "floating" electrically. The height difference ( $\Delta h$ ) between the OPA reservoir and the

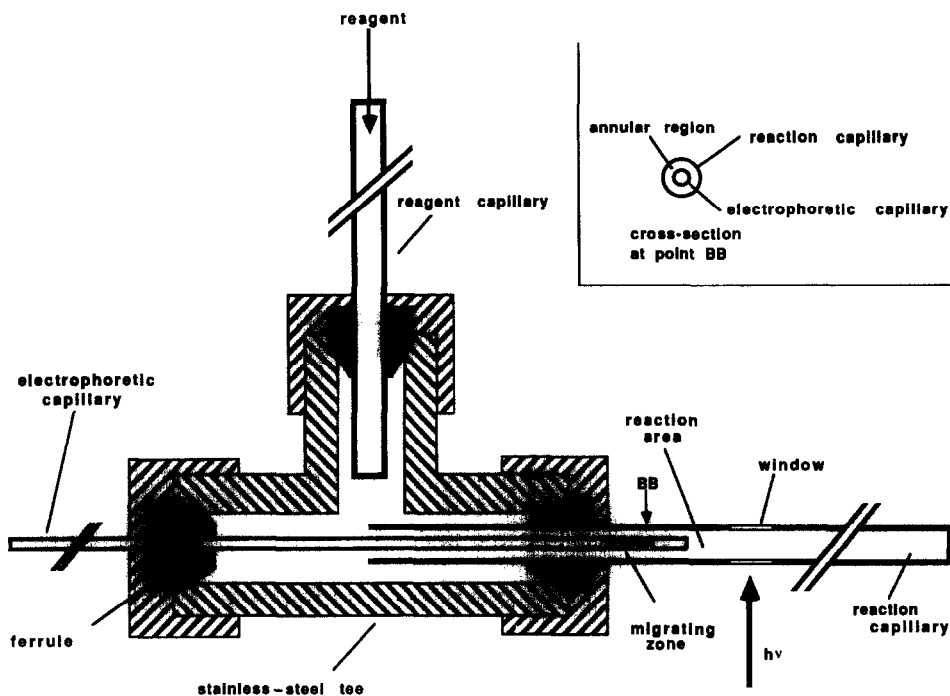


Fig. 1. Cross-sectional schematic of post-capillary reactor in stainless-steel tee.

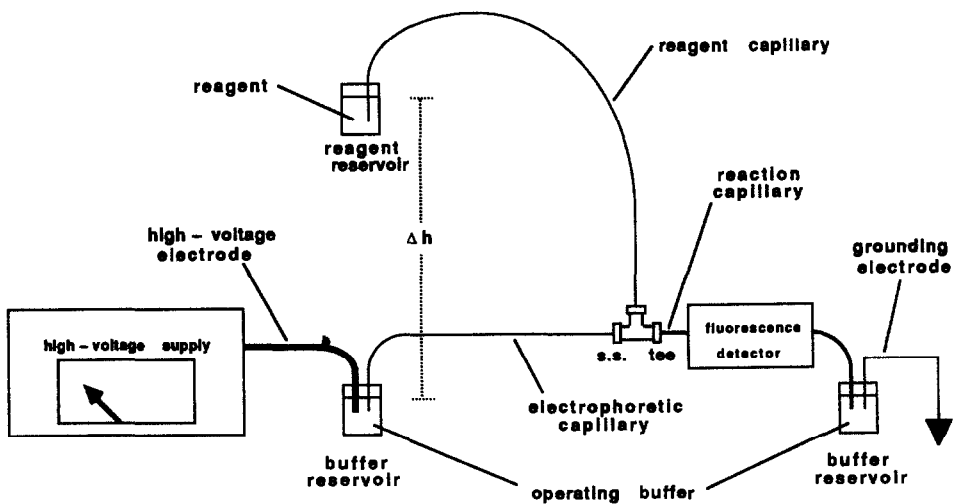


Fig. 2. Overall CZE experimental set-up for post-capillary fluorescence detection.

buffer reservoirs creates hydrostatic pressure which forces OPA reagent to flow into the tee and pass through the annular region of the coaxial reactor. A zone migrating from the tip of the electrophoretic capillary mixes with the OPA reagent in the reaction area to form a fluorescent product (see Fig. 1). Reaction products are carried a short distance (1–2 cm) “downstream” and detected by fluorescence.

#### *Instrumentation*

The apparatus for electrophoresis was similar to that previously published<sup>5,24,25</sup>. A  $\pm 30$ -kV d.c. power supply (Spellman High Voltage Electronics; Plainview, NY, U.S.A.), used in the positive voltage mode, drove the electrophoretic separations. A high-pressure mercury–xenon arc lamp source in a variable-wavelength fluorescence detector<sup>2</sup> was used with 312 nm as the excitation wavelength and two 400-nm cut-on filters for isolating the emission wavelength. The cell block of the detector was modified slightly to support the stainless-steel tee of the post-capillary reactor. Fluorescence intensity was measured using an R-212 photomultiplier tube (Hamamatsu; Middlesex, NJ, U.S.A.) and a photometer (Pacific Instruments; Concord, MA, U.S.A.) connected to the analog-to-digital converter of a multi-function interface board (Scientific Solutions, Solon, OH, U.S.A.) which was mounted in an IBM PC/XT microcomputer (IBM, Boca Raton, FL, U.S.A.). Analog conversions were made at a rate of 1 or 2 points per second.

#### *Reagents and samples*

High purity *o*-phthaldialdehyde, 2-mercaptoethanol, N-tris(hydroxymethyl)-methyl glycine (tricine), 3-(cyclohexylamino)-1-propanesulfonic acid (CAPS), 2-(N-cyclohexylamino)ethanesulfonic acid (CHES), amino acids, whale skeletal muscle myoglobin, bovine erythrocyte carbonic anhydrase, chicken egg ovalbumin and bovine milk  $\beta$ -lactoglobulin were purchased from Sigma (St. Louis, MO, U.S.A.). Bromocresol purple, boric acid, potassium hydroxide, potassium chloride, and absolute ethanol were reagent grade. Distilled water was used for all buffers.

The OPA reagent was made fresh daily by dissolving 5 mg of OPA (mol.wt. 134.1) in 50  $\mu$ l of 2-mercaptoethanol plus 200  $\mu$ l of absolute ethanol and then diluted up to 4 ml with buffer (see table footnotes and figure legends for specific buffers).

#### *Procedure*

The capillaries for the reactor were used as supplied except in cases where the outer diameter of the electrophoretic capillary was reduced using the following etching procedure: (i) the polyimide plastic coating was burned off over the desired length, (ii) water was forced through the capillary using helium pressure, and (iii) the capillary was dipped into a stirred bath of concentrated (48%) hydrofluoric acid for a specified time.

Insertion of the electrophoretic capillary into the reaction capillary to form the coaxial post-capillary reactor was done manually with the aid of a microscope and then the capillary combination was secured in the stainless-steel tee. The reactor was mounted in the detector with the reaction capillary secured in the detector block and the tee resting in a plexiglass holder attached to the block. A vacuum, applied to the end of the reaction capillary, filled the electrophoretic capillary with operating buffer, the reagent capillary with OPA reagent, and the reaction capillary with a mixture of operating buffer and OPA reagent. The vacuum was applied until no air bubbles passed through the reaction capillary, indicating that no leaks were present in the

reactor and OPA reagent completely filled the void volume of the tee. After returning the reaction capillary to the buffer reservoir, the OPA reservoir was raised to a specified height to begin reagent flow. The high voltage was applied until a flat baseline from background fluorescence was achieved.

Introduction of sample into the electrophoretic capillary was accomplished using the following procedure: (i) the OPA reservoir was lowered to the height of the buffer reservoirs, (ii) the high voltage was turned off, (iii) the end of the electrophoretic capillary was moved from buffer reservoir to sample vial (the high-voltage electrode dipped into both sample vial and buffer reservoir), (iv) the voltage was applied for a specific amount of time to migrate sample into the end of the electrophoretic capillary, (v) the end of the electrophoretic capillary was moved back to the buffer reservoir, (vi) the high voltage was applied to begin the run, and (vii) the OPA reservoir was raised to its original height. After the run, the fluorescence intensity was plotted as a function of time to produce an electropherogram. The peak limits were marked arbitrarily and a statistical moments calculation<sup>26,27</sup> was done between the marks to give peak parameters such as peak area, variance, and the number of theoretical plates ( $N$ ).

To examine mixing in the coaxial reactor, the stainless-steel tee was removed from the detector and mounted next to an optical stereomicroscope such that the tip of the electrophoretic capillary in the reaction capillary window was in the microscope's field of view. A basic solution (pH 10) of bromocresol purple, a pH indicator, was migrated through the electrophoretic capillary in a continuous zone while a basic buffer (no bromocresol purple) flowed through the reagent capillary. With this configuration, the purple solution could be seen as it emerged from the tip of the electrophoretic capillary and mixed with the basic buffer flowing from the annular region of the coaxial reactor. In a second experiment, an acidic buffer was used in the reagent capillary to change the emerging purple to yellow to help reveal the extent of mixing in the reaction area.

## RESULTS AND DISCUSSION

Characterization of post-capillary reactor. The coaxial capillary configuration was chosen for post-capillary detection in CZE because the OPA reagent could easily be introduced and mixed with a zone without the need for a mixing tee or reaction coil. The schematic in Fig. 3 shows a zone migrating from the tip of the electrophoretic capillary and mixing with the OPA reagent stream. Mixing of zone molecules and OPA reagent is due to diffusion, convection, and migration effects.

Radial diffusion occurs as analyte molecules emerge from the capillary tip and diffuse outward toward the walls of the reaction capillary, while OPA reagent diffuses into the zone. The time required for this radial diffusion can be estimated using the Einstein equation for diffusion,

$$x = (2Dt)^{1/2}$$

where  $x$  is the diffusion distance,  $D$  is the diffusion coefficient and  $t$  is the mean time required for a molecule to diffuse the distance  $x$ . Solving for the diffusion time,  $t$ , a small molecule ( $D = 1 \cdot 10^{-5} \text{ cm}^2 \text{ s}^{-1}$ ) would require 0.08 s to diffuse radially from the center to the edge of a 25- $\mu\text{m}$  wide "cylinder" of fluid emerging from the end of an

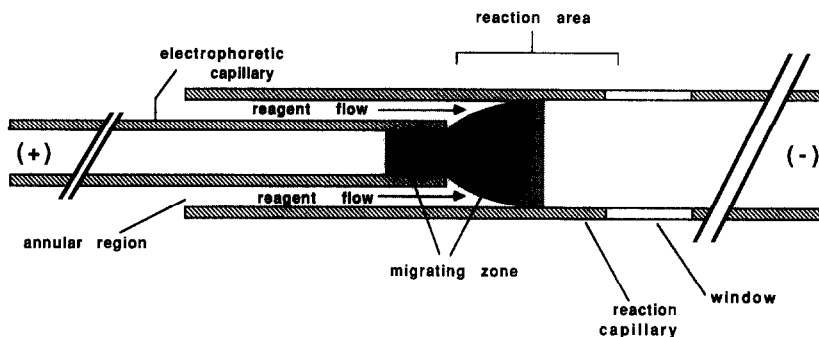


Fig. 3. Schematic of reaction area with a zone migrating from the tip of an electrophoretic capillary.

electrophoretic capillary of 25- $\mu\text{m}$  I.D. (This diffusion time increases approximately ten-fold for larger molecules such as proteins). Because OPA reagent also diffuses into the cylinder of fluid emerging from the electrophoretic capillary, the time required for OPA reagent to mix with a zone will be even less than this rough calculation indicates. Turbulent convection, if it is present, will further speed this mixing process.

A final mechanism contributing to mixing of the analyte and reagent concerns the electric field. In CZE, ions are responsible for carrying current from the high-voltage electrode through the capillary to the grounded electrode. In the post-capillary reactor, the inner diameter changes in going from electrophoretic to reaction capillary. For this reason, both buffer and analyte ions will migrate radially in order to carry current over the full cross-sectional area of the reaction capillary (see Fig. 3). This phenomenon may help to carry charged analyte molecules outward and into the flowing stream of OPA reagent which facilitates mixing.

Even though thorough mixing of an emerging zone and the OPA reagent is necessary to achieve a maximum yield of fluorescent product, mixing is also a potential source of zone broadening and must be controlled to preserve high efficiency separations. To assess the effect of post-capillary reactor mixing on zone broadening, zones were monitored at two locations. A UV absorbance detector was positioned before the stainless-steel tee such that a portion of the electrophoretic capillary formed the detector cell. Also, zones were monitored after the stainless-steel tee, in the coaxial reactor, using post-capillary fluorescence labelling. Table I compares the peak efficiencies ( $N$ ), a measure of zone width, at these two detection locations as a function of height difference,  $\Delta h$ , between the OPA reservoir and the two buffer reservoirs (see Fig. 2). An increase in the height difference causes an increase in the hydrostatic pressure resulting in an increase in the OPA reagent flow through the annular region of the capillary reactor. The data for post-capillary detection show that as the flow of OPA reagent increases, the efficiency (number of theoretical plates) increases and the peak area decreases. The inverse relationship between efficiency and peak area exists because a high flow-rate increases dilution of the zone migrating from the end of the electrophoretic capillary (thus reducing signal) but also sweeps analyte through the detection region more rapidly and thus prevents excessive residence time in the reaction area (increased efficiency). This effect was seen visually by continuously migrating a purple solution from the tip of the electrophoretic capillary (see

TABLE I

## ZONE BROADENING EFFECTS OF POST-CAPILLARY REACTOR

Conditions: operating and OPA buffer 10 mM tricine + 20 mM potassium chloride, pH 8.3; sample,  $1 \cdot 10^{-4}$  M tyrosine; sample introduction, 5 s at 15 kV; operating current 3  $\mu$ A, electrophoretic capillary, 60 cm  $\times$  150  $\mu$ m O.D.  $\times$  25  $\mu$ m I.D.; reaction capillary, 325- $\mu$ m O.D., 200- $\mu$ m I.D.

| $\Delta h$ (cm)* | Detection location                                  |                                      |             |
|------------------|---|--------------------------------------|-------------|
|                  | Electrophoretic capillary<br>(absorbance): <i>N</i> | Reaction capillary<br>(fluorescence) |             |
|                  |   | <i>N</i>                             | Peak area** |
| 2                | 15 200  | 1400                                 | 13 800      |
| 4                | 10 100  | 4400                                 | 5200        |
| 8                | 10 600  | 8700                                 | 1400        |
| 16               | 13 500  | 10 600                               | 500         |

\* Height difference between OPA reservoir and buffer reservoirs.

\*\* Arbitrary units.

Experimental section for details). At low OPA reagent flow-rates, the solution would have a profile similar to that shown in Fig. 3 whereas at higher flow-rates, the profile would be confined to a narrow stream emerging from the tip of the electrophoretic capillary.

#### Effect of post-capillary reactor dimensions

In an effort to increase the fluorescence signal and decrease zone broadening, a series of post-capillary reactors were constructed from capillaries with varying dimensions. The 25- $\mu$ m I.D. dimension of the electrophoretic capillary was kept constant throughout the study. Each capillary combination is shown in Table II and briefly described below (the combinations are represented by the notation O.D.<sub>tip</sub>/I.D.<sub>RC</sub> where O.D.<sub>tip</sub> is the tip outer diameter of the electrophoretic capillary and I.D.<sub>RC</sub> is the inner diameter of the reaction capillary).

**150/200.** This capillary combination was used for the data shown in Table I and represents the post-capillary reactor initially characterized in the previous section. The electrophoretic capillary was used as supplied without modification. The 150- $\mu$ m O.D. electrophoretic capillary was easily inserted into the 200- $\mu$ m I.D. reaction capillary to form this combination.

**36/200.** The tip of the electrophoretic capillary was tapered from 150- $\mu$ m O.D. to 36- $\mu$ m O.D. over the last 0.25 cm by etching the outside of the capillary with hydrofluoric acid. The tapered tip was an effort to reduce any turbulence due to the blunt tip of a 150- $\mu$ m O.D. electrophoretic capillary. Such turbulence was observed microscopically during continuous migration of the purple indicator from the tip of the electrophoretic capillary of the 150/200 capillary combination previously described (see Experimental section for details).

**110/160.** By burning off the polyimide plastic coating over the last 8 cm of the

TABLE II

## CAPILLARY COMBINATIONS FOR POST-CAPILLARY REACTOR

See text for explanation of each combination; reaction capillary length is 32 cm for all combinations, O.D.<sub>RC</sub> is 350  $\mu\text{m}$  for all combinations except 40/50 which was 150  $\mu\text{m}$ .

| Capillary combination* | Tip O.D. <sub>EC</sub> ( $\mu\text{m}$ )** | Nominal I.D. <sub>RC</sub> ( $\mu\text{m}$ )*** | I.D. <sub>RC</sub> - O.D. <sub>tip</sub> ( $\mu\text{m}$ ) | I.D. <sub>RC</sub> - I.D. <sub>EC</sub> ( $\mu\text{m}$ ) |
|------------------------|--|---|--|---|
| 150/200                | 150  | 200   | 50   | 175   |
| 36/200                 | 150 to 36                                  | 200   | 50 to 164  | 175   |
| 110/160                | 110  | 160   | 50   | 135   |
| 70/100                 | 70   | 100   | 30   | 75  |
| 40/50                  | 40   | 50  | 10   | 25  |

\* Electrophoretic capillary nominal I.D. = 25  $\mu\text{m}$ , O.D. = 150  $\mu\text{m}$  (unmodified) for all combinations.

\*\* Tip is terminal 8 cm of electrophoretic capillary (EC) as determined using a measuring microscope. Tip for 36/200 combination is tapered from 150  $\mu\text{m}$  to 36  $\mu\text{m}$  over terminal 0.25 cm.

\*\*\* Nominal inner diameter of reaction capillary as supplied by the manufacturer.

electrophoretic capillary, the outer diameter of the tip was reduced by approximately 35  $\mu\text{m}$ . This electrophoretic capillary was inserted into a 160- $\mu\text{m}$  I.D. reaction capillary. (Assembly of this and subsequent capillary combinations required careful

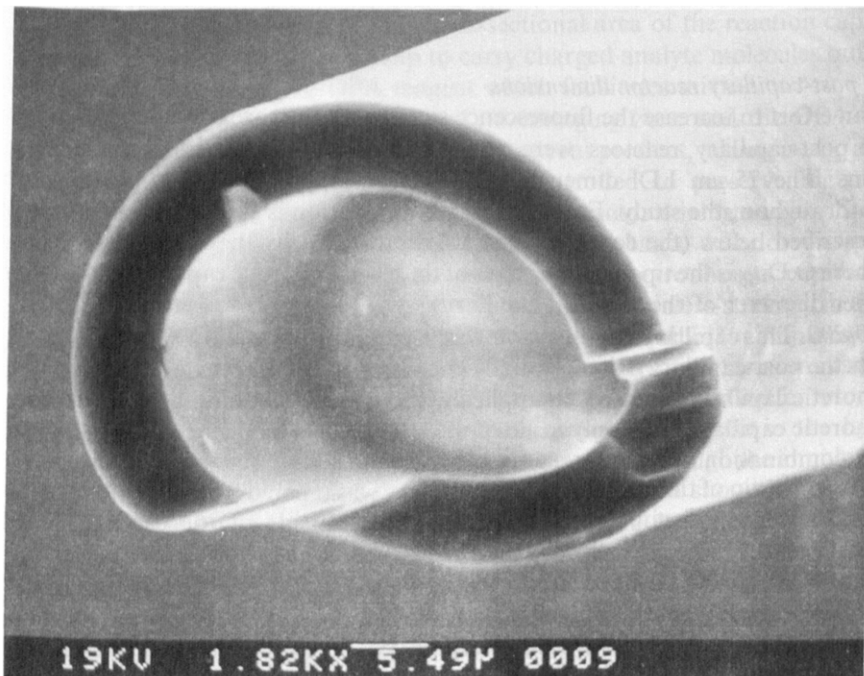


Fig. 4. Scanning electron micrograph of electrophoretic capillary tip used in 40/50 capillary combination.



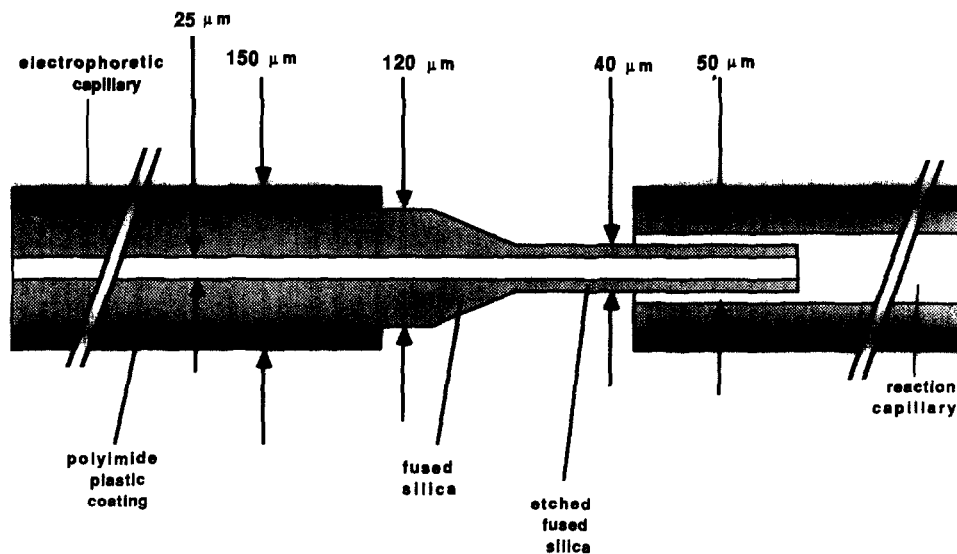


Fig. 5. Schematic of 40/50 capillary combination.

manipulation because of the fragile nature of the exposed fused silica of the electrophoretic capillary.)

*70/100 and 40/50.* Further reductions in the outer diameter of the electrophoretic capillary were achieved by burning off the polyimide plastic coating as with the

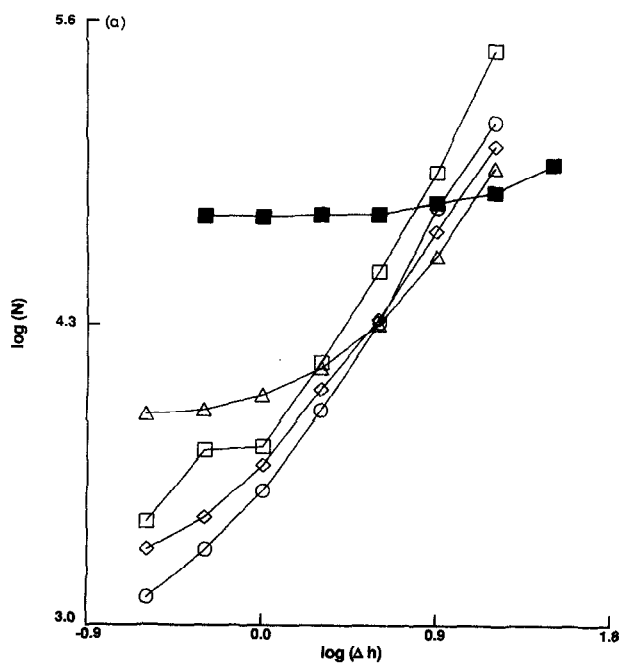


Fig. 6.

(Continued on p. 126)

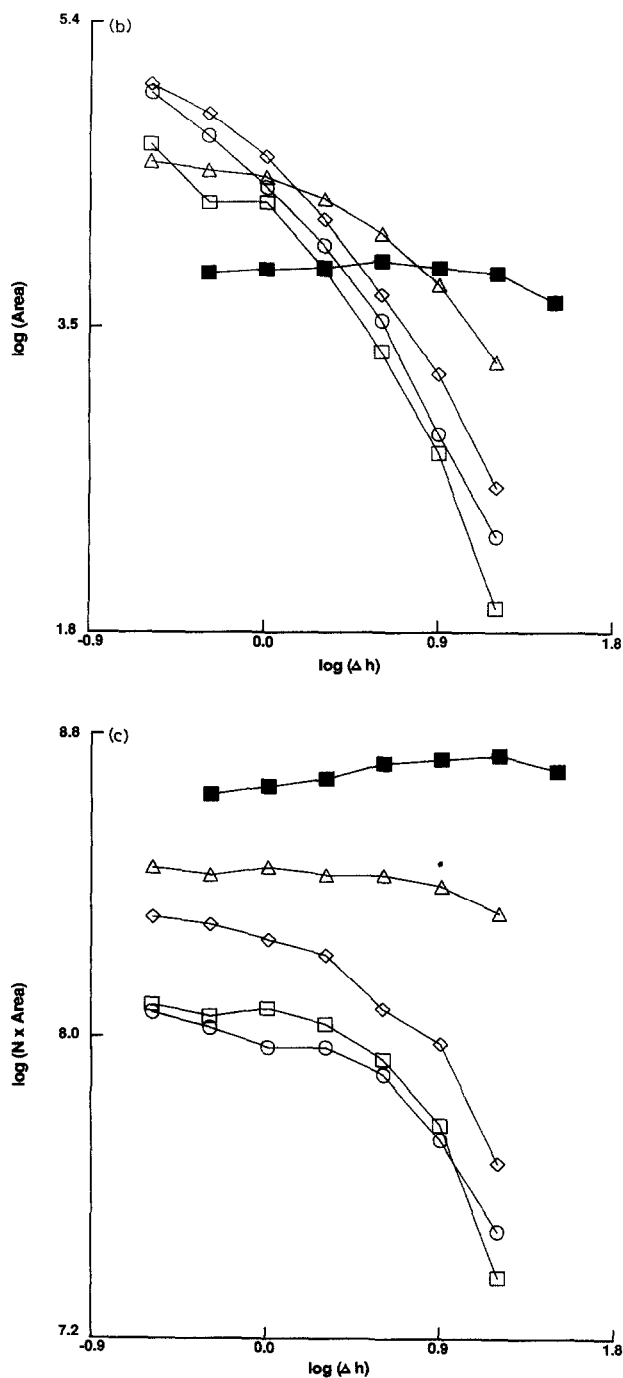


Fig. 6. Comparison of capillary combinations for a series of OPA reagent flow-rates ( $\Delta h$  in cm): 150/200 (○), 36/200 (□), 110/160 (◇), 70/100 (△), 40/50 (■). (a) log (peak efficiency,  $N$ ) vs. log ( $\Delta h$ ); (b) log (peak area) vs. log ( $\Delta h$ ); (c) log ( $N \times \text{area}$ ) vs. log ( $\Delta h$ ); operating and OPA reagent buffers, 10 mM tricine + 20 mM potassium chloride pH 8.4; test analyte,  $1 \cdot 10^{-4}$  M glycine.

110/160 combination and then etching the entire length of bare fused silica in a hydrofluoric acid bath for 15–25 min (see Experimental section for details). Fig. 4 shows an scanning electron micrograph of an etched electrophoretic capillary used in the 40/50 combination. Fig. 5 shows a schematic of the two capillaries of the 40/50 combination. In assembling this combination, care was taken to make sure that the reaction capillary was not blocked with the shoulder of the electrophoretic capillary. By reducing the outer diameter of the electrophoretic capillary to 70  $\mu\text{m}$  and to 40  $\mu\text{m}$ , correspondingly smaller reaction capillaries of 100  $\mu\text{m}$  and 50  $\mu\text{m}$  outer diameter, respectively, could be used (see Table II).

In Fig. 6, a comparison is made between these capillary combinations used for the post-capillary reactor in terms of number of theoretical plates,  $N$ , (Fig. 6a), area (Fig. 6b), and the product of  $N$  and peak area (Fig. 6c) for a series of OPA reagent flow-rates,  $\Delta h$ . In Fig. 6a and b, the 40/50 combination shows little OPA reagent flow-rate dependence as compared to the other combinations. As the difference between the inner diameters of the electrophoretic and reaction capillaries is reduced (see the 6th column of Table II), the efficiency–peak area product increases, as shown in Fig. 6c. The 40/50 combination, showing the largest efficiency–peak area product, differs in inner diameters by only 25  $\mu\text{m}$  compared to the 150/200 combination which differs in inner diameters by 175  $\mu\text{m}$ . Since a large efficiency–peak area product is desirable, the 40/50 combination was chosen as the working coaxial capillary dimension and used for the subsequent sensitivity studies and applications described below.

#### *Linearity and limits of detection*

The linearity of the post-capillary detector was evaluated from a log–log plot of peak area as a function of sample concentration. The post-capillary detector is linear over 3.5 orders of magnitude for the amino acid glycine (slope = 0.972, correlation coefficient = 0.9996). For the two proteins, whale skeletal muscle myoglobin (WSM) and carbonic anhydrase (CAH), linearity was more difficult to measure as they are more prone to exhibiting concentration dependent asymmetries in the electrophoretic process. This peak distortion made accurate measurement of peak areas difficult. This problem was further aggravated by impurities appearing as shoulders on the main protein peak. At the lower protein concentrations (less than 0.1% w/v) protein response was linear.

Fig. 7, an electropherogram of  $5 \cdot 10^{-7}$  M glycine, shows a peak representing 42 fg (560 attomol) of glycine. Using the criterion of three times the RMS noise in Fig. 7, the limit of detection is 6.3 fg (83 attomol) of glycine introduced into the electrophoretic capillary. Fig. 8, an electropherogram of 0.0001% (w/v) whale skeletal muscle myoglobin or one part per million (ppm), shows a peak representing 1.6 pg (93 attomol) of protein. Using the same criteria as described for glycine, the limit of detection is 380 fg (22.1 attomol or thirteen million molecules) of myoglobin introduced into the electrophoretic capillary.

A comparison between the relative sensitivity of post-capillary fluorescence detection and on-line UV detection is shown in Fig. 9. Fig. 9a is an electropherogram of a mixture of proteins detected using post-capillary fluorescence detection. Fig. 9b is an electropherogram of the same mixture of proteins (identical amount injected) detected using a fixed-wavelength (229 nm) UV detector<sup>1</sup> such that the length to the

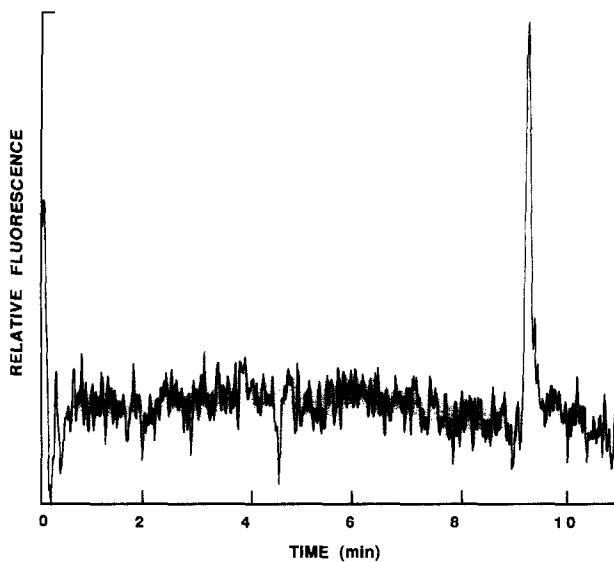


Fig. 7. Electropherogram of glycine. Peak represents 42 fg (560 attomol) glycine introduced into the capillary; data has been subjected to a nine-point Savitsky-Golay smooth<sup>28</sup>. Operating and OPA reagent buffer, 50 mM borate + 50 mM potassium chloride, pH 9.5. Sample introduction, 2 s at 30 kV; operating voltage, 30 kV;  $\Delta h = 16$  cm.

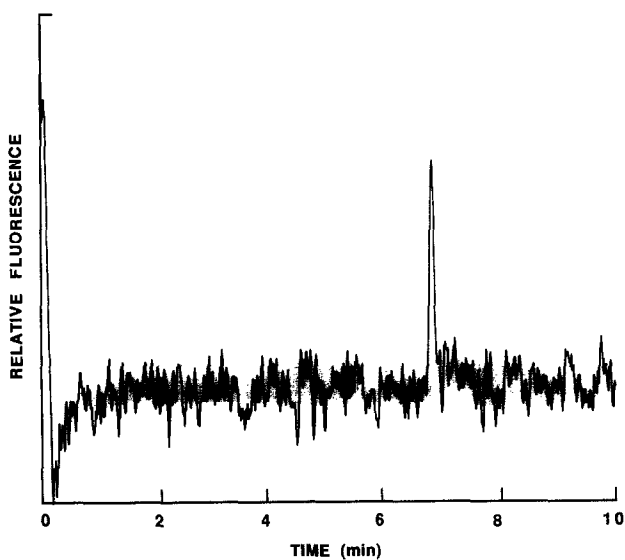


Fig. 8. Electropherogram of whale skeletal muscle myoglobin. Peak represents 1.6 pg (93 attomol) myoglobin introduced into the capillary; data has been subjected to a nine-point Savitsky-Golay smooth<sup>28</sup>; for operating conditions, see Fig. 7.

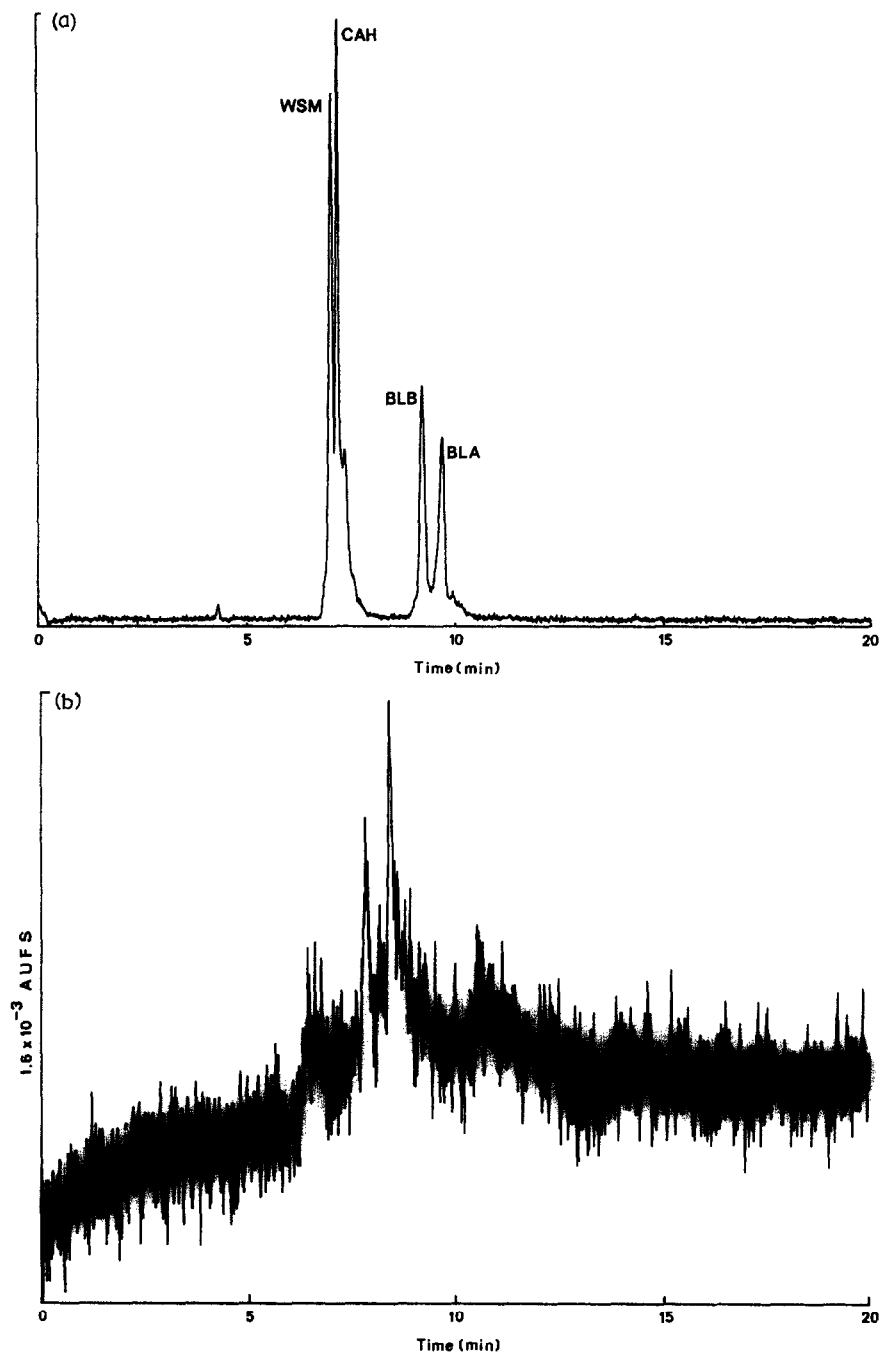


Fig. 9. Comparison of post-capillary fluorescence and UV detection of 0.01% (w/v) whale skeletal muscle myoglobin (WSM), 0.01% (w/v) carbonic anhydrase (CAH), 0.005% (w/v)  $\beta$ -lactoglobulin B (BLB), 0.005% (w/v)  $\beta$ -lactoglobulin A (BLA). (a) Post-capillary fluorescence detection; (b) UV (229 nm) detection; operating and OPA reagent buffer, 50 mM borate + 50 mM potassium chloride, pH 9.5. For operating conditions, see Fig. 7.

on-line detection window was the same as the length of the electrophoretic capillary in the post-capillary scheme (all other electrophoretic parameters such as injection/run voltage and time were the same for both runs). The improvement in signal-to-noise is approximately 100-fold using the post-capillary fluorescence detection.

Detection using post-capillary OPA derivatization affords the analysis of a variety of samples with amine-containing samples. Fig. 10 shows the separation and detection of amine-containing compounds in red wine. This figure points to the advantages of post-capillary fluorescence detection in CZE. The sample required no sample preparation other than a four-fold dilution. Also, because the detection scheme responds only to primary amines, it is more selective than UV detection, for example. This selectivity, combined with the sensitivity of fluorescence detection, enables the quantification of the minor component, histamine, in a complex sample.

A post-capillary fluorescence detection system for CZE has been described which uses no mixing tee or loops in which to react electrophoretic zones with OPA reagent. The detection limits for this system represent a major improvement over any detection scheme suitable for protein detection previously described for CZE. This detection scheme is useful for the analysis of amine-containing biomolecules in complex mixtures.

The work described herein points to several areas of improvement which would further enhance this detection system. Use of a laser as the excitation source (as opposed to the arc lamp used here) should increase the fluorescence intensity of the

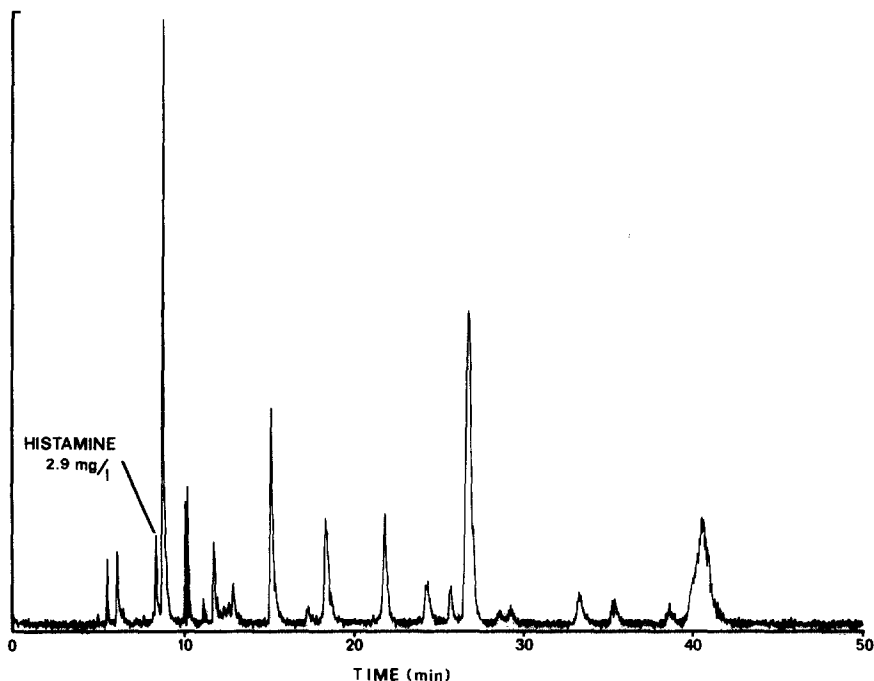


Fig. 10. Electropherogram of red wine (1984 Fonset-Lacour Bordeaux), four-fold dilution of unfiltered sample with operating buffer; operating buffer, 100 mM borate + 200 mM potassium chloride, pH 9.5; OPA reagent buffer 0.1 M CAPS, pH 11.0.  $\Delta h = 32$  cm; sample introduction, 2 s at 30 kV; run voltage, 25 kV.

OPA adduct. Pumping of OPA reagent using a constant flow pump would allow precise quantitation and control of reagent flow-rate and increase the reliability of reagent flow into the reaction area. Finally, replacement of the stainless-steel tee union with a cross union would provide a more effective means of flushing out the void volume of the union with fresh OPA reagent daily.

#### ACKNOWLEDGEMENTS

Support for this work was provided by the Hewlett-Packard Corporation, and by the National Science Foundation under Grant CHE-8607899.

#### REFERENCES

- 1 Y. Walbroehl and J. W. Jorgenson, *J. Chromatogr.*, 315 (1984) 135.
- 2 J. S. Green and J. W. Jorgenson, *J. Chromatogr.*, 352 (1986) 337.
- 3 P. Gozel, E. Gassman, H. Michelsen and R. N. Zare, *Anal. Chem.*, 59 (1987) 44.
- 4 K. D. Lukacs, *Ph.D. Dissertation*, University of North Carolina, Chapel Hill, NC, 1983.
- 5 X. Huang, T. J. Pang, M. J. Gordon and R. N. Zare, *Anal. Chem.*, 59 (1987) 2747.
- 6 F. E. P. Mikkers, F. M. Everaerts and Th. P. E. M. Verheggen, *J. Chromatogr.*, 169 (1979) 11.
- 7 F. Foret, M. Deml, V. Kahle and P. Boček, *Electrophoresis*, 7 (1986) 430.
- 8 J. A. Olivares, N. T. Nguyen, C. R. Yonker and R. D. Smith, *Anal. Chem.*, 59 (1987) 1230.
- 9 R. A. Wallingford and A. G. Ewing, *Anal. Chem.*, 59 (1987) 1762.
- 10 K. Muramoto, H. Kawauchi, Y. Yamamoto and K. Tuzimura, *Agric. Biol. Chem.*, 40 (1976) 815.
- 11 K. Muramoto, H. Kamiya and H. Kawauchi, *Anal. Biochem.*, 141 (1984) 446.
- 12 K. Samejima, *J. Chromatogr.*, 96 (1974) 250.
- 13 K. Imai, *J. Chromatogr.*, 105 (1975) 135.
- 14 V. T. Wiedmeier, S. P. Porterfield and C. E. Hendrich, *J. Chromatogr.*, 231 (1982) 410.
- 15 Y. Tapuhi, N. Miller and B. L. Karger, *J. Chromatogr.*, 205 (1981) 325.
- 16 H. Umagat, P. Kucera and L.-F. Wen, *J. Chromatogr.*, 239 (1982) 463.
- 17 M. J. Winspear and A. Oaks, *J. Chromatogr.*, 270 (1983) 378.
- 18 V. A. Fried, M. E. Ando and A. J. Bell, *Anal. Biochem.*, 146 (1985) 217.
- 19 R. W. Frei, L. Michel and W. Santi, *J. Chromatogr.*, 126 (1976) 665.
- 20 P. Bohlen, S. Stein, J. Stone and S. Udenfreind, *Anal. Biochem.*, 67 (1975) 438.
- 21 P. Kucera and H. Umagat, *J. Chromatogr.*, 255 (1983) 563.
- 22 H. P. M. van Vliet, G. J. M. Bruin, J. C. Kraak and H. Poppe, *J. Chromatogr.*, 363 (1986) 187.
- 23 P. Lindroth and K. Mopper, *Anal. Chem.*, 51 (1979) 1667.
- 24 J. W. Jorgenson and K. D. Lukacs, *Anal. Chem.*, 53 (1981) 1298.
- 25 J. W. Jorgenson and K. D. Lukacs, *Science (Washington, D.C.)*, 222 (1983) 266.
- 26 L. B. Rogers and J. E. Oberholtzer, *Anal. Chem.*, 41 (1969) 1234.
- 27 O. Grubner, *Anal. Chem.*, 43 (1971) 1934.
- 28 A. Savitsky and M. J. E. Golay, *Anal. Chem.*, 36 (1964) 1627.